Commun. Comput. Phys.
doi: 10.4208/cicp.020415.260717a

Vol. **23**, No. 2, pp. 500-519
February 2018

A Finite Volume Method for the Relativistic Burgers Equation on a FLRW Background Spacetime

Tuba Ceylan[1], Philippe G. LeFloch[2,*] and Baver Okutmustur[1]

[1] *Department of Mathematics, Middle East Technical University (METU), 06800 Ankara, Turkey.*
[2] *Laboratoire Jacques-Louis Lions & Centre National de la Recherche Scientifique, Université Pierre et Marie Curie (Paris 6), 4 Place Jussieu, 75252 Paris, France.*

Communicated by Chi-Wang Shu

Received 2 April 2015; Accepted (in revised version) 26 July 2017

Abstract. A relativistic generalization of the inviscid Burgers equation was introduced by LeFloch and co-authors and was recently investigated numerically on a Schwarzschild background. We extend this analysis to a Friedmann-Lemaître-Robertson-Walker (FLRW) background, which is more challenging due to the existence of time-dependent, spatially homogeneous solutions. We present a derivation of the model of interest and we study its basic properties, including the class of spatially homogeneous solutions. Then, we design a second-order accurate scheme based on the finite volume methodology, which provides us with a tool for investigating the properties of solutions. Computational experiments demonstrate the efficiency of the proposed scheme for numerically capturing weak solutions.

AMS subject classifications: 35L65, 76N10, 83A05

Key words: Relativistic Burgers equation, FLRW metric, hyperbolic balance law, finite volume scheme.

1 Introduction

Aim of this paper

The inviscid Burgers equation is an important model in computational fluid dynamics and provides the simplest (yet challenging) example of a nonlinear hyperbolic conservation law. Recently, a relativistic generalization of the standard Burgers equation was introduced on curved spacetimes and studied by LeFloch and collaborators [1–4,9–12]. This

*Corresponding author. *Email addresses:* ceylanntuba@gmail.com (T. Ceylan), contact@philippelefloch.org (P. G. LeFloch), baver@metu.edu.tr (B. Okutmustur)

relativistic Burgers equation, as it is now called, takes into account geometrical effects and satisfies the Lorentz invariance property, also enjoyed by the Euler equations of relativistic compressible fluids. In LeFloch, Makhlof, and Okutmustur [11], this model was studied on a Schwarzschild black hole background and a numerical scheme was designed from the finite volume methodology which allowed one to capture weak solutions containing shock waves. The standard maximum principle and the total variation diminishing (TVD) principle are lacking for Burgers-type equations on a curved geometry, so that it necessary to revisit standard approaches if stable approximation schemes are sought for. Our main objective in the present paper is to extend the results in [11] and design an accurate and robust numerical scheme when the model of interest is formulated on a cosmological background and, especially, on a Friedmann-Lemaître-Robertson-Walker (FLRW) geometry. This latter spacetime is a solution to Einstein's field equations and is particularly relevant in cosmology [7].

The relativistic Burgers equations on a curved background

Our model is derived from the full relativistic Euler equations posed on a smooth, time-oriented Lorentzian manifold (M,g), that is,

$$\nabla_\alpha T^{\alpha\beta}=0, \qquad T^{\alpha\beta}=(\rho c^2+p)\,u^\alpha u^\beta+p\,g^{\alpha\beta},$$

where $T^{\alpha\beta}$ is the energy-momentum tensor of a perfect fluid. Here, $\rho\geq 0$ denotes the mass-energy density of the fluid, while the future-oriented, unit timelike vector field $u=(u^\alpha)$ represents the fluid velocity, normalized to be unit: $g_{\alpha\beta}u^\alpha u^\beta=-1$.

As usual, the Euler equations are supplemented with an equation of state for the pressure $p=p(\rho)$. In the present work, we assume that the fluid is pressureless, that is, $p\equiv 0$, so that the Euler system takes the simpler form

$$\nabla_\alpha\left(\rho u^\alpha u^\beta\right)=0. \tag{1.1}$$

Provided ρ,u are sufficiently regular, we can write

$$\rho\nabla_\alpha u^\alpha u^\beta+\rho u^\alpha\nabla_\alpha u^\beta+u^\alpha u^\beta\nabla_\alpha\rho=0.$$

By contracting this equation with the covector u_β and by observing[†] that $g_{\alpha\beta}u^\beta\nabla_\gamma u^\alpha=0$, we get $u^\alpha\nabla_\alpha\rho=-\rho\nabla_\alpha u^\alpha$. In turn, from (1.1) it follows that

$$\rho u^\beta\nabla_\alpha u^\alpha+\rho u^\alpha\nabla_\alpha u^\beta-\rho u^\beta\nabla_\alpha u^\alpha=0.$$

Finally, provided $\rho>0$, it follows that

$$u^\alpha\nabla_\alpha u^\beta=0, \tag{1.2}$$

which we refer to as the *relativistic Burgers equation* (expressed here in a non-divergence form) on a curved background (M,g). Its unknown is the vector field (u^β) satisfying the normalization $g_{\alpha\beta}u^\alpha u^\beta$.

[†] u is orthogonal to ∇u, as is easily checked by differentiating the identity $g_{\alpha\beta}u^\alpha u^\beta=-1$ stating that u is unit vector and by recalling that ∇ is the Levi-Civita connection associated with the metric $g_{\alpha\beta}$ so that $\nabla_\gamma g_{\alpha\beta}=0$.

Minkowski and Schwarzschild backgrounds

Recall that the standard inviscid Burgers equation is one of the simplest example of a nonlinear hyperbolic conservation law and reads

$$\partial_t v+\partial_x(v^2/2)=0, \tag{1.3}$$

where the unknown $v=v(t,x)$ is defined for $t\geq 0$ and $x\in\mathbb{R}$. This equation can be derived[‡] from the Euler system of compressible fluids

$$\begin{aligned}&\partial_t\rho+\partial_x(\rho v)=0,\\&\partial_t(\rho v)+\partial_x(\rho v^2+p(\rho))=0,\end{aligned}$$

where $p(\rho)$ denotes the pressure of the fluid and ρ denotes its density. By assuming a pressureless fluid $p(\rho)\equiv 0$ and keeping a suitable combination of the two equations above, we can obtain (1.3). Namely, we have

$$\begin{aligned}0&=v\partial_t(\rho)+\rho\partial_t(v)+v^2\partial_x(\rho)+2v\rho\partial_x v=\rho(\partial_t v+2v\partial_x v)+v(\partial_t\rho+v\partial_x\rho)\\&=\rho(\partial_t v+2v\partial_x v)-v\rho\partial_x v=\rho(\partial_t v+v\partial_x v)\end{aligned}$$

and, provided the density does not vanish, we get $\partial_t v+v\partial_x v=0$, which is equivalent to (1.3).

We recall that LeFloch et al. [11] treated the relativistic version (1.2) on Minkowski or Schwarzschild backgrounds. We recall that the relativistic Burgers equation on the flat Minkowski spacetime derived in (1.2) can also be characterized by imposing the Lorentz invariance property. On a Schwarzschild spacetime, the Burgers equations is found to be

$$\partial_t(r^2v)+\partial_r\Big(r(r-2m)\frac{v^2}{2}\Big)=rv^2-mc^2, \tag{1.4}$$

where the Schwarzschild metric in coordinates (t,r,θ,φ) is defined by

$$g=-\Big(1-\frac{2m}{r}\Big)c^2dt^2+\Big(1-\frac{2m}{r}\Big)^{-1}dr^2+r^2(d\theta^2+\sin^2 d\varphi^2), \tag{1.5}$$

so that $m>0$ is the mass parameter, c is the light speed, r is the Schwarzschild radius and $r>2m$. We refer the reader to [11] for further details. The Schwarzschild metric represents the geometry of a *static* black hole and, consequently, Eq. (1.4) admits an important family of explicit solutions, i.e. the family of time-independent solutions.

Outline of this paper

In Section 2, we discuss the FLRW geometry and express the pressureless Euler system on a FLRW background. Then, in Sections 3 and 4, we present the derivation of the Burgers

[‡]formally, at least

equation which is the equation of main interest in this paper. We are in a position in Section 5 to study the family of spatially homogeneous solutions and then in Section 6 we design the finite volume scheme we propose in this paper. Finally, Section 7 contains various numerical experiments and in Section 8 we end with several remarks.

2 The compressible Euler system on a FLRW background

FLRW metrics

We work with the FLRW metric describing a spatially homogeneous and isotropic three-dimensional space. In term of the proper time t measured by a co-moving observer, a radial variable r, and angular θ,φ measured in the co-moving frame, the metric reads

$$g=-c^2dt^2+a(t)^2\Big(\frac{dr^2}{1-kr^2}+r^2d\theta^2+r^2\sin^2\theta d\varphi^2\Big), \tag{2.1}$$

where $a=a(t)$ is a function (see next paragraph) and $k=0,\pm1$. The variable t is the cosmological proper time experienced by observers who remain at rest in co-moving coordinates and observes a uniform expansion of the surrounding Universe.

The function a is taken to be of the form $a(t)=a_0\big(\frac{t}{t_0}\big)^\alpha$ and, for the FLRW metric, one has $\alpha=\frac{2}{3}$, in which t_0 represents the age of the Universe. The constant parameter k is related to the spacetime curvature K by the relation $k=a(t)^2K$ and we distinguish between three cases:

$$k=\begin{cases}1, & \text{sphere (of positive curvature)},\\ 0, & \text{(flat) Euclidean space (of vanishing curvature)},\\ -1, & \text{hyperboloid (of negative curvature)}.\end{cases} \tag{2.2}$$

Expressions in coordinates

The FLRW metric can also be written in the form

$$g=(dtdrd\theta d\varphi)\begin{pmatrix}-c^2 & 0 & 0 & 0\\ 0 & \frac{a^2}{1-kr^2} & 0 & 0\\ 0 & 0 & a^2r^2 & 0\\ 0 & 0 & 0 & a^2r^2\sin^2\theta\end{pmatrix}\begin{pmatrix}dt\\ dr\\ d\theta\\ d\varphi\end{pmatrix}$$

or else

$$g_{00}=-c^2,\quad g_{11}=\frac{a^2}{1-kr^2},\quad g_{22}=a^2r^2,\quad g_{33}=a^2r^2\sin^2\theta, \tag{2.3}$$

which are the only non-vanishing covariant components, and

$$g^{00}=-\frac{1}{c^2},\quad g^{11}=\frac{1-kr^2}{a^2},\quad g^{22}=\frac{1}{a^2r^2},\quad g^{33}=\frac{1}{a^2r^2\sin^2\theta}. \tag{2.4}$$

We will also need the expressions of the Christoffel symbols $\Gamma^{\mu}_{\alpha\beta}$. Using (2.3) and (2.4) and the definition $\Gamma^{\mu}_{\alpha\beta}=\frac{1}{2}g^{\mu\nu}(-\partial_\nu g_{\alpha\beta}+\partial_\beta g_{\alpha\nu}+\partial_\alpha g_{\beta\nu})$, where $\alpha,\beta,\mu,\nu\in\{0,1,2,3\}$, we first calculate

$$\Gamma^0_{00}=\frac{1}{2}g^{00}(-\partial_0 g_{00}+\partial_0 g_{00}+\partial_0 g_{00})=0, \tag{2.5}$$

and then

$$\begin{aligned}\Gamma^0_{11}&=\frac{1}{2}g^{00}(-\partial_0 g_{11}+\partial_1 g_{10}+\partial_0 g_{10})\\&=\frac{1}{2}(-1)\Big(-\partial_0\Big(\frac{a^2}{(1-kr^2)}\Big)\Big)=\frac{a\dot{a}}{c(1-kr^2)}.\end{aligned} \tag{2.6}$$

Similarly, we can compute the other non-vanishing Christoffel symbols and conclude that

$$\begin{aligned}&\Gamma^0_{11}=\frac{a\dot{a}}{c(1-kr^2)},\qquad \Gamma^0_{22}=\frac{a\dot{a}r^2}{c},\qquad \Gamma^0_{33}=\frac{a\dot{a}r^2\sin^2\theta}{c},\\&\Gamma^1_{11}=\frac{kr}{1-kr^2},\qquad \Gamma^1_{22}=-r(1-kr^2),\qquad \Gamma^1_{33}=-r(1-kr^2)\sin^2\theta,\\&\Gamma^2_{33}=-\sin\theta\cos\theta,\qquad \Gamma^3_{23}=\Gamma^3_{32}=\cot\theta,\quad \Gamma^2_{12}=\Gamma^2_{21}=\Gamma^3_{31}=\Gamma^3_{13}=\frac{1}{r},\\&\Gamma^1_{01}=\Gamma^1_{10}=\Gamma^2_{02}=\Gamma^2_{20}=\Gamma^3_{30}=\Gamma^3_{03}=\frac{\dot{a}}{ca}.\end{aligned} \tag{2.7}$$

The energy-momentum tensor for perfect fluids

We consider a fluid flow evolving on a FRLW background and assume that solutions to the Euler equations depend only on the time variable t and the radial variable r, and that the non-radial components of the velocity vanish, that is, $(u^\alpha)=(u^0(t,r),u^1(t,r),0,0)$. Since u is unit vector, we have $u^\alpha u_\alpha=-1$ and we write

$$u^\alpha u_\alpha=u^0u_0+u^1u_1=g_{00}(u^0)(u^0)+g_{11}(u^1)(u^1),$$

which gives $-1=g_{00}(u^0)^2+g_{11}(u^1)^2$. It follows that

$$-1=-c^2(u^0)^2+\frac{a(t)^2}{1-kr^2}(u^1)^2. \tag{2.8}$$

It is convenient to introduce the velocity component

$$v:=\frac{ca(t)}{(1-kr^2)^{1/2}}\frac{u^1}{u^0}. \tag{2.9}$$

By using (2.8) and (2.9) with a simple algebraic manipulation, we obtain the following identities

$$(u^0)^2=\frac{c^2}{(c^2-v^2)},\qquad (u^1)^2=\frac{v^2(1-kr^2)}{a^2(c^2-v^2)}. \tag{2.10}$$

The energy momentum tensor of perfect fluids read

$$T^{\alpha\beta}=(\rho c^2+p)\,u^\alpha u^\beta+p g^{\alpha\beta}. \tag{2.11}$$

Combining (2.4) with (2.10) and (2.11), we obtain the components of the energy momentum tensor:

$$\begin{aligned}
&T^{00}=(\rho c^2+p)u^0u^0+pg^{00}=\frac{c^2}{c^2-v^2}(\rho c^2+p)-p=\frac{\rho c^4+pv^2}{c^2-v^2},\\
&T^{01}=T^{10}=\frac{cv(1-kr^2)^{1/2}(\rho c^2+p)}{a(c^2-v^2)},\qquad T^{11}=\frac{c^2(1-kr^2)(v^2\rho+p)}{a^2(c^2-v^2)},\\
&T^{22}=\frac{p}{a^2r^2},\qquad T^{33}=\frac{p}{a^2r^2\sin^2\theta}.
\end{aligned} \tag{2.12}$$

The pressureless Euler system on a FLRW background

We are in a position to derive the Euler system $\nabla_\alpha T^{\alpha\beta}=0$ on a FLRW spacetime:

$$\partial_\alpha T^{\alpha\beta}+\Gamma^\alpha_{\alpha\gamma}T^{\gamma\beta}+\Gamma^\beta_{\alpha\gamma}T^{\alpha\gamma}=0. \tag{2.13}$$

Taking first $\beta=0$, (2.13) yields

$$\partial_\alpha T^{\alpha0}+\Gamma^\alpha_{\alpha\gamma}T^{\gamma0}+\Gamma^0_{\alpha\gamma}T^{\alpha\gamma}=0,$$

which is equivalent to

$$\begin{aligned}
&\partial_0T^{00}+\Gamma^0_{0\gamma}T^{\gamma0}+\Gamma^0_{\gamma0}T^{\gamma0}+\partial_1T^{10}+\Gamma^1_{1\gamma}T^{\gamma0}+\Gamma^0_{1\gamma}T^{1\gamma}+\partial_2T^{20}+\Gamma^2_{2\gamma}T^{\gamma0}\\
&\quad+\Gamma^0_{2\gamma}T^{2\gamma}+\partial_3T^{30}+\Gamma^3_{3\gamma}T^{\gamma0}+\Gamma^0_{3\gamma}T^{3\gamma}=0.
\end{aligned}$$

Next consider $\beta=1$, that is, $\partial_\alpha T^{\alpha1}+\Gamma^\alpha_{\alpha\gamma}T^{\gamma1}+\Gamma^1_{\alpha\gamma}T^{\alpha\gamma}=0$, which gives us

$$\begin{aligned}
&\partial_0T^{01}+\Gamma^0_{0\gamma}T^{\gamma1}+\Gamma^0_{0\gamma}T^{0\gamma}+\partial_1T^{11}+\Gamma^1_{1\gamma}T^{\gamma1}+\Gamma^1_{1\gamma}T^{1\gamma}+\partial_2T^{21}+\Gamma^2_{2\gamma}T^{\gamma1}\\
&\quad+\Gamma^1_{2\gamma}T^{2\gamma}+\partial_3T^{31}+\Gamma^3_{3\gamma}T^{\gamma1}+\Gamma^1_{3\gamma}T^{3\gamma}=0.
\end{aligned}$$

We substitute the expressions (2.7) of the Christoffel symbols and obtain

$$\begin{aligned}
&\partial_0T^{00}+\partial_1T^{10}+\frac{3\dot a}{ca}T^{00}+\frac{kr}{1-kr^2}T^{10}+\frac{a\dot a}{c(1-kr^2)}T^{11}\\
&\qquad+\frac{2}{r}T^{10}+\frac{r^2a\dot a}{c}T^{22}+\frac{a\dot ar^2\sin^2\theta}{c}T^{33}=0,\\
&\partial_0T^{01}+\partial_1T^{11}+\frac{4\dot a}{ca}T^{01}+\frac{\dot a}{ca}T^{10}+\frac{2kr}{(1-kr^2)}T^{11}\\
&\qquad+\frac{1}{r}T^{11}-r(1-kr^2)T^{22}-r(1-kr^2)\sin^2\theta T^{33}=0.
\end{aligned} \tag{2.14}$$

Finally, using the expressions (2.12) for perfect fluids into and assuming that the pressure p vanishes identically, we obtain the *compressible Euler system on a FLRW background:*

$$\partial_0\left(\frac{\rho c^2}{c^2-v^2}\right)+\partial_1\left(\frac{\rho cv(1-kr^2)^{1/2}}{a(c^2-v^2)}\right)+\frac{3\dot{a}\rho c^2}{a(c^2-v^2)}+\frac{2\rho cv(1-kr^2)^{1/2}}{ra(c^2-v^2)}$$
$$+\frac{kr\rho cv}{a(c^2-v^2)(1-kr^2)^{1/2}}+\frac{\dot{a}v^2\rho}{ca(c^2-v^2)}=0, \tag{2.15}$$

$$\partial_0\left(\frac{c\rho v(1-kr^2)^{1/2}}{a(c^2-v^2)}\right)+\partial_1\left(\frac{v^2\rho(1-kr^2)}{a^2(c^2-v^2)}\right)+\frac{5\dot{a}\rho vc(1-kr^2)^{1/2}}{a^2(c^2-v^2)}$$
$$+\frac{2krv^2\rho}{a^2(c^2-v^2)}+\frac{2v^2\rho(1-kr^2)}{ra^2(c^2-v^2)}=0. \tag{2.16}$$

3 The relativistic Burgers equation on a FLRW background

The derivation of the relativistic Burgers equation

We now derive the relativistic Burgers equation from the system (2.15)-(2.16). First of all, from (2.15) we express $\partial_0\left(\frac{\rho c^2}{c^2-v^2}\right)$ as

$$\partial_0\left(\frac{\rho c^2}{c^2-v^2}\right)=-\partial_1\left(\frac{\rho cv(1-kr^2)^{1/2}}{a(c^2-v^2)}\right)-\frac{3\dot{a}\rho c}{a(c^2-v^2)}-\frac{2\rho cv(1-kr^2)^{1/2}}{ra(c^2-v^2)}$$
$$-\frac{kr\rho cv}{a(c^2-v^2)(1-kr^2)^{1/2}}-\frac{\dot{a}v^2\rho}{ca(c^2-v^2)}.$$

Next, we take partial derivatives in (2.16) and get

$$\partial_0\left(\frac{c^2\rho}{c^2-v^2}\right)\left(\frac{v(1-kr^2)^{1/2}}{a}\right)+\left(\frac{c^2\rho}{c^2-v^2}\right)\partial_0\left(\frac{v(1-kr^2)^{1/2}}{a}\right)$$
$$+\partial_1\left(\frac{cv\rho(1-kr^2)^{1/2}}{a(c^2-v^2)}\right)\left(\frac{v(1-kr^2)^{1/2}}{a}\right)$$
$$+\left(\frac{cv\rho(1-kr^2)^{1/2}}{a(c^2-v^2)}\right)\partial_1\left(\frac{v(1-kr^2)^{1/2}}{a}\right)$$
$$+\frac{5\dot{a}\rho vc(1-kr^2)^{1/2}}{a^2(c^2-v^2)}+\frac{2krcv^2\rho}{a^2(c^2-v^2)}+\frac{2cv^2\rho(1-kr^2)}{ra^2(c^2-v^2)}=0.$$

Then, we substitute the expression $\partial_0\left(\frac{\rho c^2}{c^2-v^2}\right)$ and find

$$\begin{aligned}
&\partial_1\left(\frac{\rho cv(1-kr^2)^{1/2}}{a(c^2-v^2)}\right)+\frac{3\dot{a}\rho c}{a(c^2-v^2)}+\frac{2\rho cv(1-kr^2)^{1/2}}{ra(c^2-v^2)}+\frac{kr\rho cv}{a(c^2-v^2)(1-kr^2)^{1/2}}\\
&\quad+\frac{\dot{a}v^2\rho}{ca(c^2-v^2)}\left(\frac{v(1-kr^2)^{1/2}}{a}\right)+\left(\frac{c^2\rho}{c^2-v^2}\right)\partial_0\left(\frac{v(1-kr^2)^{1/2}}{a}\right)\\
&\quad+\partial_1\left(\frac{cv\rho(1-kr^2)^{1/2}}{a(c^2-v^2)}\right)\left(\frac{v(1-kr^2)^{1/2}}{a}\right)+\left(\frac{cv\rho(1-kr^2)^{1/2}}{a(c^2-v^2)}\right)\partial_1\left(\frac{v(1-kr^2)^{1/2}}{a}\right)\\
&\quad+\frac{5\dot{a}\rho vc(1-kr^2)^{1/2}}{a^2(c^2-v^2)}+\frac{2krcv^2\rho}{a^2(c^2-v^2)}+\frac{2cv^2\rho(1-kr^2)}{ra^2(c^2-v^2)}=0.
\end{aligned}\tag{3.1}$$

After further calculations and replacing the notation (∂_t,∂_r) by (∂_0,∂_1), we arrive at

$$a^2\partial_t\left(\frac{v}{a}(1-kr^2)^{1/2}\right)+\partial_r\left(\left(\frac{v^2}{2}\right)(1-kr^2)\right)+v(1-kr^2)^{1/2}a_t\left(2-\frac{v^2}{c^2}\right)+rkv^2=0.\tag{3.2}$$

It follows that

$$(av_t-va_t)(1-kr^2)^{1/2}+(1-kr^2)\partial_r\left(\frac{v^2}{2}\right)-rkv^2+v(1-kr^2)^{1/2}a_t\left(2-\frac{v^2}{c^2}\right)+rkv^2=0$$

and, after simplification,

$$av_t(1-kr^2)^{1/2}+(1-kr^2)\partial_r\left(\frac{v^2}{2}\right)+v\left(1-kr^2\right)^{1/2}a_t\left(1-\frac{v^2}{c^2}\right)=0.$$

Definition 3.1. The *relativistic Burgers equation on a FLRW background* is the following balance law

$$av_t+\left(1-kr^2\right)^{1/2}\partial_r\left(\frac{v^2}{2}\right)+v\left(1-\frac{v^2}{c^2}\right)a_t=0\tag{3.3}$$

with unknown $v=v(t,r)$, in which the function $a=a(t)>0$ is given, $k\in\{-1,0,1\}$ is a discrete parameter, and the light speed c is a positive parameter.

The physical parameters of interest

In (3.3), we are especially interested in the physically relevant expression

$$a(t)=a_0\left(\frac{t}{t_0}\right)^{\alpha}\tag{3.4}$$

for some given t_0, so that the relativistic Burgers equation depends upon the following parameters:

$$\begin{array}{ll}
k\in[-1,1] & \text{is the curvature constant,}\\
c\in(0,\infty) & \text{is the light speed,}\\
a_0\in(0,\infty) & \text{is the scaling factor,}\\
\alpha\in(0,\infty) & \text{is the scale exponent.}
\end{array}\tag{3.5}$$

Two main ranges of the time variable are relevant in the problem under consideration. Since shock wave solutions to nonlinear hyperbolic equations can only be defined *in forward time directions* (due to the entropy condition and the implied irreversibility property) and since the equation is singular at $t=0$, we distinguish between two regimes:

(1) In the range $t\in[1,\infty)$, we use the normalization $t_0=1$ and the spacetime is *expanding toward the future*.

(2) In the range $t\in[-1,0)$, we use the normalization $t_0=-1$ and the spacetime is *contracting toward the future*.

Basic properties

Eq. (3.3) is a nonlinear hyperbolic equation with time- and space-dependent coefficients. The solutions admit jump discontinuities which may arise from an initially smooth data and propagate in time. Kruzkov's theory of entropy weak solutions applies immediately to the Cauchy problem. In the special case $a(t)\equiv 1$ and $k\equiv 0$, we recover the standard Burgers equation and entropy solutions are known to satisfy the maximum principle

$$\inf_y v(0,y)\leq v(t,x)\leq \sup_y v(0,y) \quad \text{for all relevant values } (t,x).$$

For general a and k, this maximum principle *does not hold* and this is one of the main challenges in dealing with (3.3) and designing efficient schemes for the computation of shock wave solutions.

Observe that, in the non-relativistic limit $c\to+\infty$, Eq. (3.3) converges to

$$\partial_t\Big(\frac{a(t)v}{(1-kr^2)^{1/2}}\Big)+\partial_r\Big(\frac{v^2}{2}\Big)=0, \tag{3.6}$$

which, in this limiting regime, leads us to a *conservation law*. On the other hand, if we keep c finite but suppress the effect of the geometry by choosing $a(t)\equiv 1$, then Eq. (3.3) also takes the form of a *conservation law*, i.e.

$$\partial_t\Big(\frac{v}{(1-kr^2)^{1/2}}\Big)+\partial_r\Big(\frac{v^2}{2}\Big)=0. \tag{3.7}$$

Spatially homogeneous solutions

It is natural to seek first for special classes of solutions to (3.3). Due to the presence of the coefficient $a(t)$ which depend on t (unless it is chosen to be constant), the only *time-independent solution* is $v\equiv 0$.

On the other hand, the class of *spatially homogeneous solutions* of (3.3) is richer. Assuming that v depends on t only, we see that the term $\partial_r(\frac{v^2}{2})$ vanishes identically and thus

$$av_t+v\Big(1-\frac{v^2}{c^2}\Big)a_t=0.$$

This yields us

$$\Big(\frac{1}{v}+\frac{\frac{v}{c^2}}{1-\frac{v^2}{c^2}}\Big)v_t=-(\log a)_t,$$

hence $\frac{\pm v}{\sqrt{1-v^2/c^2}}=\frac{w}{a}$, where w is a constant.

Claim 1. The spatially homogeneous solutions $v=v(t)$ to the relativistic Burgers equation on a FLRW background are given by

$$v(t)=\frac{w}{\sqrt{a(t)^2+\frac{w^2}{c^2}}}\in(-c,c) \tag{3.8}$$

and are parametrized by a single real parameter w.

The non-relativistic limit

As mentioned earlier, by taking the limit $c\to+\infty$ in Eq. (3.3), we obtain

$$\partial_t(av)+(1-kr^2)^{1/2}\frac{1}{2}\partial_r(v^2)=0. \tag{3.9}$$

We can also determine directly the limiting behavior of the spatially homogeneous solutions to (3.3): in view of (3.8), we obtain

$$v(t)=\frac{1}{\sqrt{\frac{1}{c^2}+\frac{a^2(t)}{w^2}}}, \tag{3.10}$$

where w is a constant parameter. Let us finally make the following observations:

- Spatially homogeneous solutions always satisfy $|v|<c$.
- In the expanding direction $t\to+\infty$, we have $v\to 0$.
- In the contraction direction $t\to 0$, we have $v\to c$ since $a(t)\to 0$.
- Furthermore, we have $v\to\frac{w}{a(t)}$ as $c\to+\infty$.

4 A finite volume method for the relativistic Burgers equation

Finite volume methodology for geometric balance laws

In Burgers equation on a FLRW background, the variable coefficients *depend upon the time variable* t, due to the terms $a(t)$, $a'(t)$ and $k\in\{-1,0,1\}$. Hence, the numerical approximation of solutions to Burgers equation on a FLRW background leads to a new challenge, in comparison to flat or Schwarzschild backgrounds.

As explained earlier, the spacetime of interest is described by a single chart and some coordinates denoted by (t,r). For the discretization, we denote the (constant) time length by Δt and we set $t_n = n\Delta t$, and we introduce equally spaced cells $I_j = [r_{j-1/2}, r_{j+1/2}]$ with (constant) spatial length $\Delta r = r_{j+1/2} - r_{j-1/2}$. The finite volume method is based on an averaging of the balance law

$$\partial_t(T^0(t,r)) + \partial_r(T^1(t,r)) = S(t,r), \tag{4.1}$$

over each grid cell $[t_n, t_{n+1}] \times I_j$, where $T^\alpha(v) = T^\alpha(t,r)$ and $S(t,r)$ are the flux and source terms, respectively. We thus have the identity

$$\begin{aligned}\int_{r_{j-1/2}}^{r_{j+1/2}} (T^0(t_{n+1},r) - T^0(t_n,r))\,dr \\ + \int_{t_n}^{t_{n+1}} (T^1(t,r_{j+1/2}) - T^1(t,r_{j-1/2}))\,dt = \int_{[t_n,t_{n+1}]\times I_j} S(t,r)\,dt\,dr\end{aligned}$$

or, by re-arranging the terms,

$$\begin{aligned}\int_{r_{j-1/2}}^{r_{j+1/2}} T^0(t_{n+1},r)\,dr = \int_{r_{j-1/2}}^{r_{j+1/2}} T^0(t_n,r)\,dr + \int_{[t_n,t_{n+1}]\times I_j} S(t,r)\,dt\,dr \\ - \int_{t_n}^{t_{n+1}} (T^1(t,r_{j+1/2}) - T^1(t,r_{j-1/2}))\,dt.\end{aligned} \tag{4.2}$$

Then, we introduce the following approximations

$$\begin{aligned}&\frac{1}{\Delta r}\int_{r_{j-1/2}}^{r_{j+1/2}} T^0(t_n,r)\,dr \simeq \overline{T}_j^n, \qquad \frac{1}{\Delta t}\int_{t_n}^{t_{n+1}} T^1(t,r_{j\pm1/2})\,dt \simeq \overline{Q}_{j\pm1/2}^n, \\ &\frac{1}{\Delta t \Delta r}\int_{[t_n,t_{n+1}]\times I_j} S(t,r)\,dt\,dr \simeq \overline{S}_j^n\end{aligned}$$

so that our scheme takes the following finite volume form

$$\overline{T}_j^{n+1} = \overline{T}_j^n - \frac{\Delta t}{\Delta r}(\overline{Q}_{j+1/2}^n - \overline{Q}_{j-1/2}^n) + \Delta t \overline{S}_j^n. \tag{4.3}$$

Keeping in mind the practical implementation of the scheme, we write also $\overline{T}_j^n = \overline{T}(v_j^n)$, where $\overline{T}$ is the (invertible) map determined by the equation. The piecewise constant approximations (v_j^n) at the "next" time level are thus given by the formula

$$v_j^{n+1} = \overline{T}^{-1}\Big(\overline{T}(v_j^n) - \frac{\Delta t}{\Delta r}(\overline{Q}_{j+1/2}^n - \overline{Q}_{j-1/2}^n) + \Delta t \overline{S}_j^n\Big). \tag{4.4}$$

For the scheme to be fully specified, we still need to select a numerical flux and an approximation of the source term.

Approximating Burgers equation on a FLRW background

Consider first he partial differential equation in conservation form

$$\partial_t v+\partial_r f(v,r)=0, \tag{4.5}$$

for which time-independent solutions have the property that $r\mapsto f(v(r),r)$ is constant in r. A general finite volume approximation for Eq. (4.5) can be written as

$$v_j^{n+1}=v_j^n-\frac{\Delta t}{\Delta r}\big(f_{j+1/2}^n-f_{j-1/2}^n\big), \tag{4.6}$$

where $f_{j+1/2}^n=f_{j+1/2}(v_j^n,v_{j+1}^n)$ is an approximation of the flux at the cell interface $r_{j+1/2}$ and such a discretization can be constructed to preserved the the family of time-independent solutions at the discrete level.

On the other hand, the relativistic Burgers equation (3.3) under consideration can be put in two different forms, that is, an equation whose the left-hand side has a nonconservative form

$$v_t+\big(1-kr^2\big)^{1/2}\frac{1}{a(t)}\partial_r\Big(\frac{v^2}{2}\Big)=-v(1-v^2)\frac{a_t(t)}{a(t)}=:S_N, \tag{4.7}$$

and on the other hand an equation whose left-hand side has a conservative form

$$\partial_t v+\partial_r\Big((1-kr^2)^{1/2}\frac{v^2}{2a(t)}\Big)=-\Big(\frac{krv^2}{2a(t)}(1-kr^2)^{-1/2}+v(1-v^2)\frac{a_t(t)}{a(t)}\Big)=:S_C. \tag{4.8}$$

Note the obvious relation $S_C=S_N+\widetilde{S}$ with $\widetilde{S}=-\frac{krv^2}{2a(t)}(1-kr^2)^{-1/2}$. The second form appears to be preferable since like in (4.5) one can take advantage of the conservation form in order to formulate the discrete scheme and make sure that the integral of the solution is preserved in time at the discrete level. A finite volume scheme for (4.8) has the general form

$$v_j^{n+1}=v_j^n-\frac{\Delta t}{\Delta r}\big(b_{j+1/2}^n g_{j+1/2}^n-b_{j-1/2}^n g_{j-1/2}^n\big)+\Delta t S_j^n, \tag{4.9}$$

in which we still need to specify the numerical flux $f_{j+1/2}^n=b_{j+1/2}^n g_{j+1/2}^n$.

The second-order Godunov-type scheme

A first-order scheme for the equation $\partial_t v+\partial_r f(v,r)=0$ and, more generally, similarly for an equation like $\partial_t v+\partial_r f(v,r)=g(v,r)$ can be turned into a second-order method by suitably "advancing" the cell-boundary values used in the numerical flux functions in order to determine the intermediate time level $t^{n+1/2}=(t^n+t^{n+1})/2$. More precisely, the second-order Godunov scheme is obtained from the edge values of the reconstructed profile advanced by half a time step. Following van Leer [15], our algorithm is formulated as follows:

- We reconstruct the solution within the computational cells by introducing values $(v^n_{i,L}, v^n_{i,R})$ in each cell, so that $v^n_{i,L}$ lies between v^n_{i-1} and v^n_i, and $v^n_{i,R}$ lies between v^n_i and v^n_{i+1}.
- We proceed to advance the solution by half a step in time. The intermediate values at the cell edges at the time $t^{n+1/2}=(t^n+t^{n+1})/2$ are denoted by $(v^n_{i,L}, v^n_{i,R})$ and are determined by

$$v^{n+1/2}_{i,L}=v^n_{i,L}-\frac{\Delta t}{2\Delta r}\big(f(v^n_{i,R},r_i)-f(v^n_{i,L},r_i)\big),$$
$$v^{n+1/2}_{i,R}=v^n_{i,R}-\frac{\Delta t}{2\Delta r}\big(f(v^n_{i,R},r_i)-f(v^n_{i,L},r_i)\big).$$

- We next solve the standard Riemann problem formed by the constant intermediate values $(v^n_{i,L}, v^n_{i,R})$. The solution $v^{n+1/2}_{i+1/2}$ is used to compute the flux $f^{n+1/2}_{i+1/2}=f(v^{n+1/2}_{i+1/2})$.
- Finally we proceed the solution by the time step Δt from t^n by using the formula

$$v^{n+1}_i=v^n_i-\frac{\Delta t}{\Delta r}\big(f^{n+1/2}_{i+1/2}-f^{n+1/2}_{i-1/2}\big).$$

  In addition, a min-max limiter (following [15]) is applied to the reconstructed values in order to avoid the formation of oscillations.

5 Numerical experiments with the relativistic Burgers equation

The first-order Godunov-type scheme

We now present several numerical experiments which are going to illustrate the main properties of the Burgers model posed on a FLRW background, as well as the properties of the proposed Godunov-type schemes. In particular, we are interested in the propagation of shock-like waves and rarefaction waves when the Godunov flux determined from a local Riemann problem is used in each grid cell. In our experiments, we choose $a(t)=t^2$ and $r\in[-1,1]$. Since our equation admits a singularity at $t=0$ stemming from the function $a(t)$, we consider the interval $t\geq 1$ for all cases of $k=-1,0,1$. In each Riemann problem, the CFL stability condition must be determined as usual from considering the fastest wave arising at each grid cell. We impose free boundary conditions at the end point of the interval. After normalization by taking $c=1$ in Eq. (3.3), we write our model as (4.8) and our finite volume scheme reads

$$v^{n+1}_j=v^n_j-\frac{\Delta t}{\Delta r}\Big(b^n_{j+1/2}\,g^n_{j+1/2}-b^n_{j-1/2}g^n_{j-1/2}\Big)+\Delta t S^n_j, \tag{5.1}$$

in which we define

$$S^n_j=-v^n_j(1-(v^n_j)^2)\frac{a^n_t}{a^n}-\frac{kr_j(v^n_j)^2}{2a^n}(1-k(r_j)^2)^{-1/2}$$

and

$$b^n_{j+1/2}=\frac{(1-k(r_{j+1/2})^2)^{1/2}}{a^n}, \qquad g^n_{j+1/2}=f(v^n_j,v^n_{j+1}),$$

where $f(u,v)$ denotes the Godunov flux function determined by solving a local Riemann problem. Here, $r_j=(1/2)\left(r_{j-1/2}+r_{j+1/2}\right)$, while $a^n=a(t_n)$ and $a^n_t=a_t(t^n)$ are known once we specify the function a. For the sake of stability, we require that the time length Δt and the space length Δr satisfy the CFL stability condition

$$\frac{\Delta t}{\Delta r}\max_j(1-k(r_j)^2)^{1/2}\frac{|v^n_j|}{a^n}<1. \tag{5.2}$$

We have implemented this first-order Godunov scheme and analyzed the dynamics of nonlinear waves arising in the problem, and in particular we compared the numerical solutions obtained in the cases $k=-1$, $k=0$, and $k=1$. These results are presented in Figs. 1 and 2. From these plots, we observe that the numerical solution for the case $k=-1$ (which is represented by the red line), moves faster than the solutions for the cases $k=0$ and $k=1$, represented by the green curve and the blue curve, respectively. We observe that, for all cases $k=-1$, $k=0$, or $k=1$, the solution converges when the mesh size is reduced.

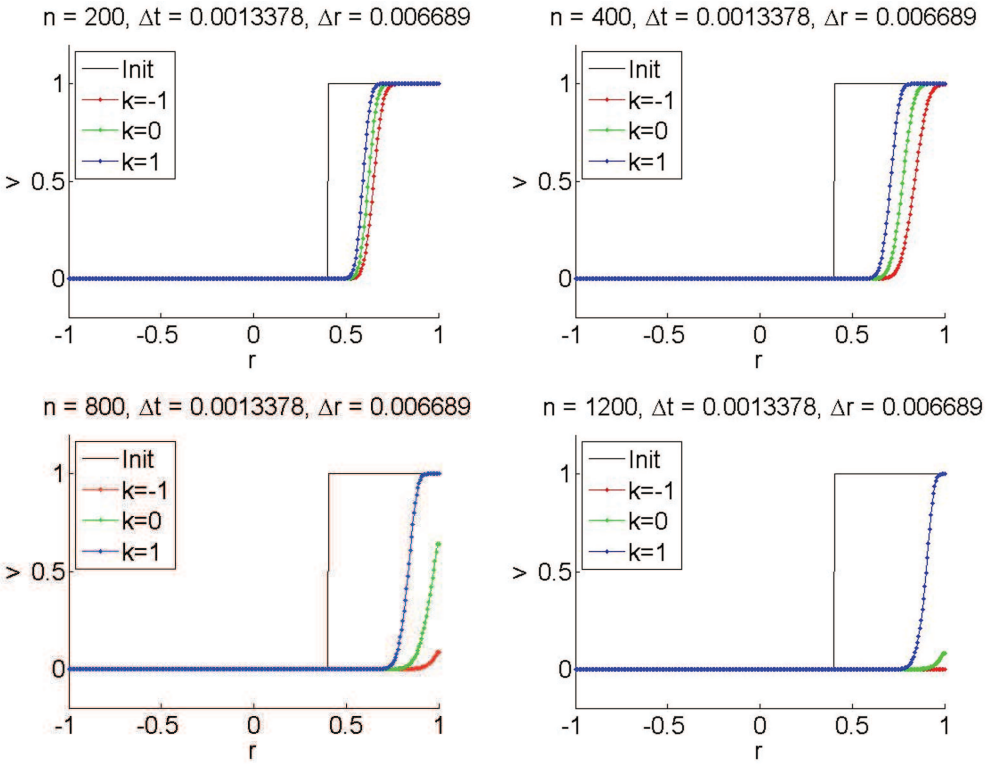

Figure 1: The first-order Godunov-type scheme for a rarefaction-like wave in the cases $k=-1$, $k=0$, and $k=1$.

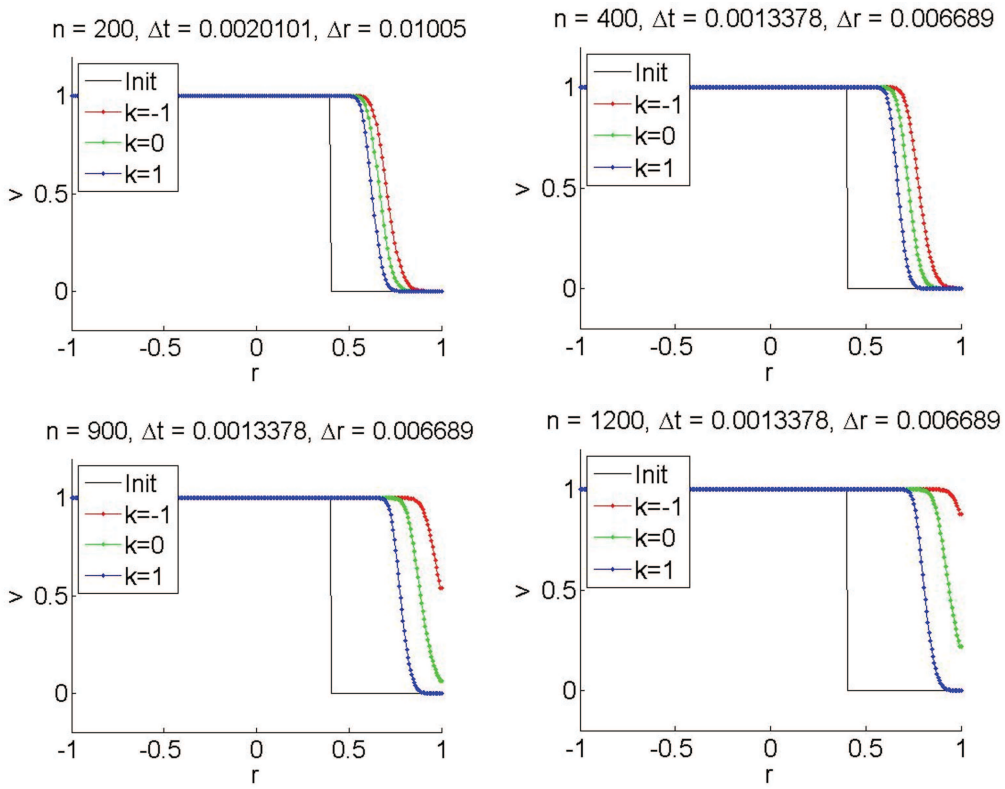

Figure 2: The first-order Godunov-type scheme for a shock-like wave in the cases $k=-1$, $k=0$, and $k=1$.

The second-order Godunov-type scheme

We now improve the accuracy by relying on our second-order Godunov-type scheme, which was describe earlier. For the implementation, we write

$$v_j^{n+1} = v_j^n - \frac{\Delta t}{\Delta r}\left(b_{j+1/2}^{n+1/2} g_{j+1/2}^{n+1/2} - b_{j-1/2}^{n+1/2} g_{j-1/2}^{n+1/2}\right) + \Delta t S_j^{n+1/2} \tag{5.3}$$

and

$$v_{j\pm1/2}^{n+1/2} = v_{j\pm1/2}^n - \frac{\Delta t}{2\Delta r}\left(b_{j+1/2}^n g_{j+1/2}^n - b_{j-1/2}^n g_{j-1/2}^n\right) + \frac{\Delta t}{2} S_{j\pm1/2}^n, \tag{5.4}$$

where $t^{n+1/2} = (t^n + t^{n+1})/2$ and

$$S_j^{n+1/2} = -v_j^{n+1/2}\left(1-(v_j^{n+1/2})^2\right)\frac{a_t^{n+1/2}}{a^{n+1/2}} - \frac{k r_j (v_j^{n+1/2})^2}{2a^{n+1/2}}(1-k(r_j)^2)^{-1/2},$$

with

$$b_{j\pm1/2}^{n+1/2} = \frac{(1-k(r_{j\pm1/2}^{n+1/2})^2)^{1/2}}{a^{n+1/2}}, \qquad g_{j-1/2}^{n+1/2} = f(v_{j-1}^{n+1/2}, v_j^{n+1/2}).$$

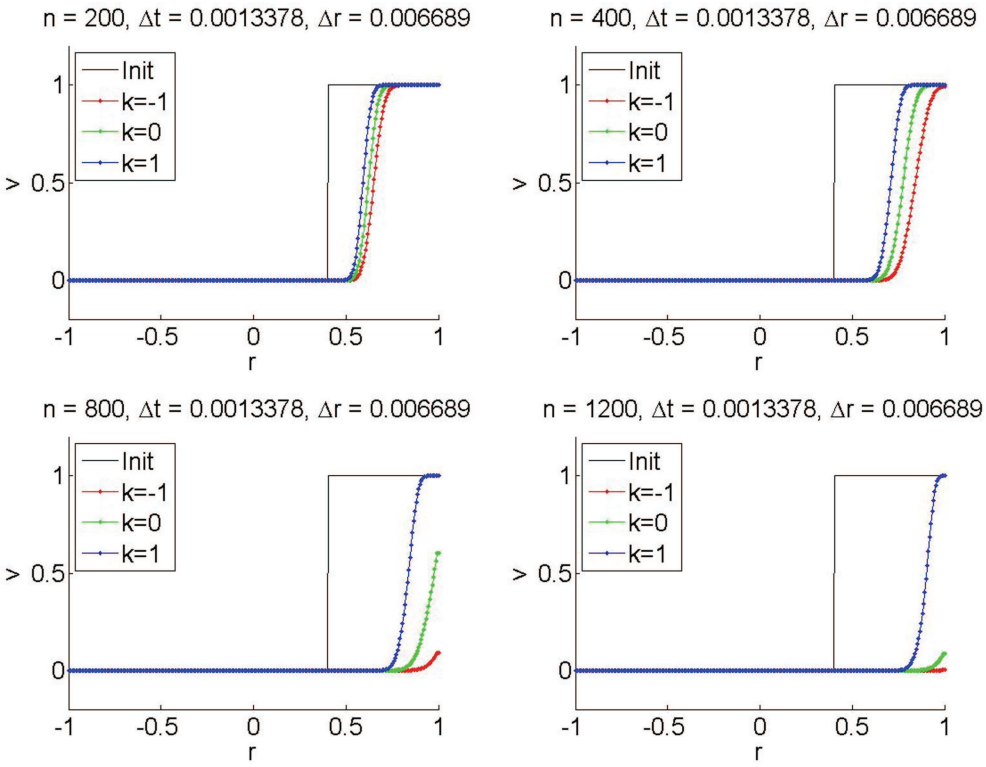

Figure 3: The second-order Godunov-type scheme for a rarefaction-like wave in the cases $k=-1$, $k=0$, and $k=1$.

The implementation of the second-order Godunov-type scheme is based on the expressions above.

In order to compare the efficiency of the first-order and second-order schemes, we repeat the same numerical tests. We deal with shock-like wave and rarefaction-like waves in Figs. 3 and 4 for the three cases of interest $k=-1$, $k=0$, and $k=1$. We observe that the second-order version significantly improves upon the first-order version. Furthermore, the numerical solution for the case $k=-1$ (represented by the red line) again moves faster than in the cases $k=0$ and $k=1$, represented by the green and blue curves, respectively.

The grid convergence

In Figs. 5 and 6, we now analyze the convergence when the mesh sizes are reduced and approach zero. We consider again the relativistic Burgers model in presence of a single wave. As mentioned earlier, the Godunov-type scheme is based on local Riemann problems at each grid interface and that the standard Riemann solver only is used for which the effect of the geometry and the source-term are suppressed.

We choose here $a(t)=t^2$ and the spatial variable describes $r\in[-1,1]$ and for definite-

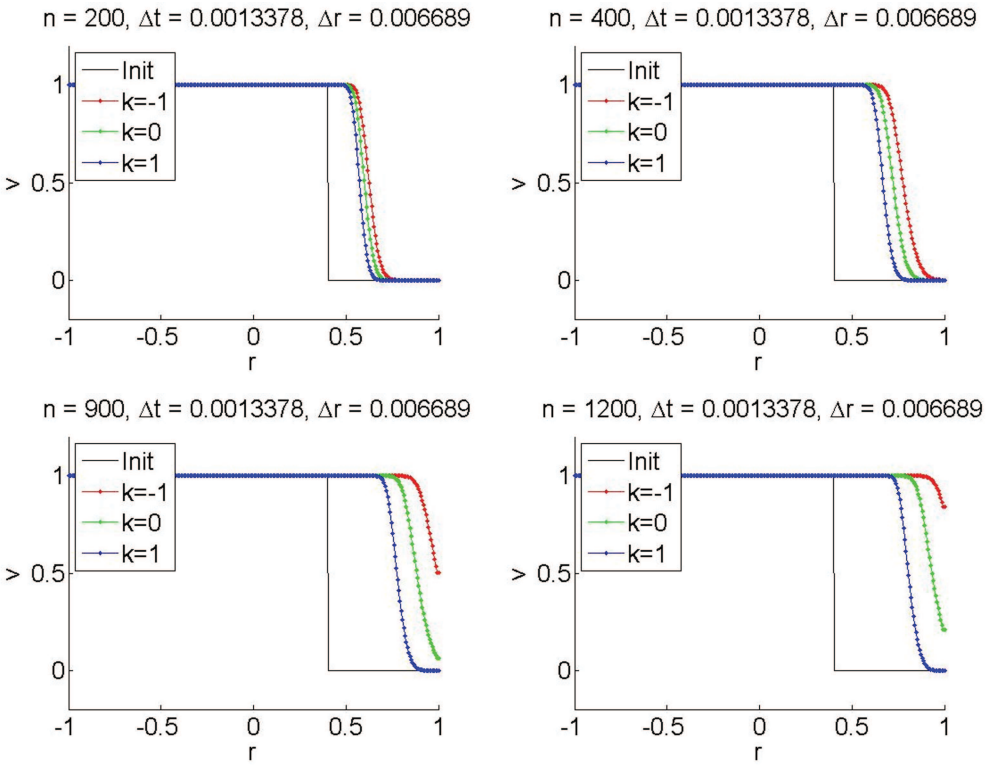

Figure 4: The second-order Godunov-type scheme for a shock-like wave in the cases $k=-1$, $k=0$, and $k=1$.

ness we take $k=1$. We use the notation J for the total number of grid cells in space and by n to indicate the total number of time steps. What we will do here is to compare the solution at low and intermediate resolution with the numerical solution obtained with a very high resolution, say corresponding to the choice $J=4000$ and $n=6000$ which provide a very fine grid for our numerical scheme and virtually coincides with the exact solution and we may view it as our "reference solution".

In Fig. 5, we compare this reference solution with the numerical solution given by the first-order Godunov-type scheme. The red curve is obtained by tour first-order scheme for $J=250,500,1000,2000$, respectively. In addition, in this figure the blue curve represents the reference solution. From this graph, it can be observed that the numerical solution represented by the red curve approaches the reference solution represented by the blue curve as J increases.

As we treat a test admitting a continuous solution, we establish our conclusion by computing the sup-norm between the blue and red curves for $J=250,500,1000$ and 2000 successively, and this sup-norm is found to be 0.4445,0.3674,0.2668,0.1412 for the mesh resolution $J=250,500,1000,2000$ respectively. Fig. 6, represents the relation between number of grid cells in space J and the error in sup-norm, and clearly demonstrates that the error decreases as J increases. Similar conclusion would be reached in the L^1 norm.

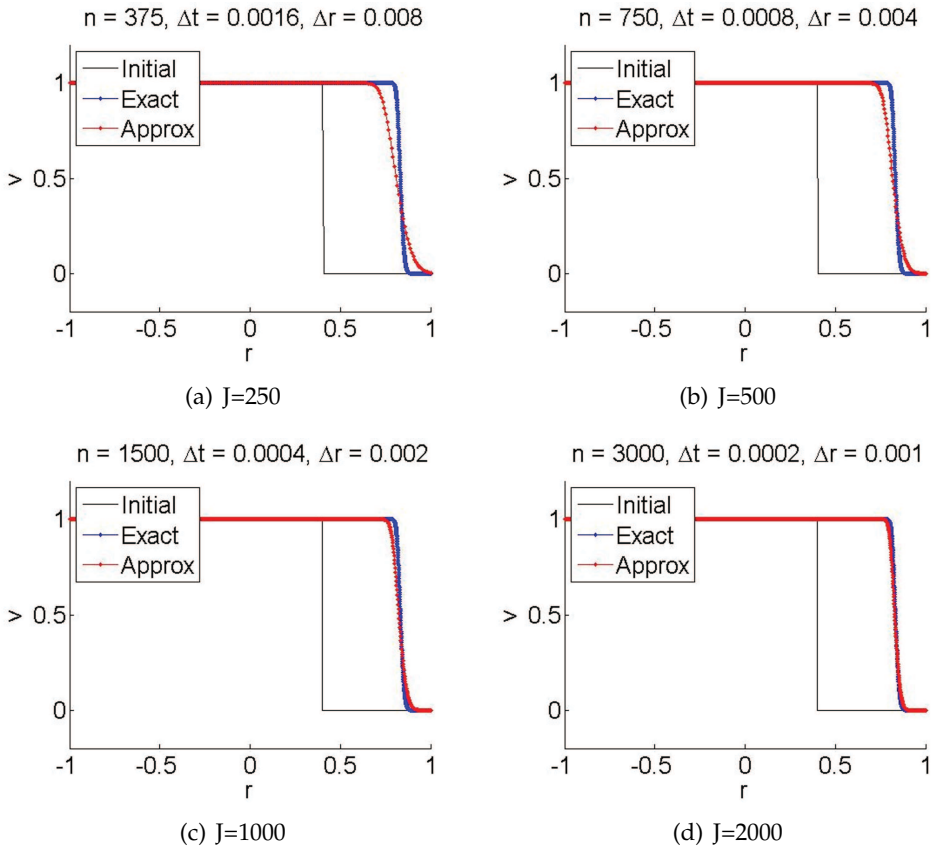

(a) J=250 (b) J=500

(c) J=1000 (d) J=2000

Figure 5: Comparing the Godunov-type solution (red line) with the reference solution (blue line, very high resolution).

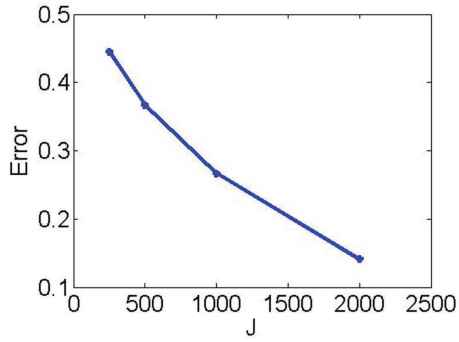

Figure 6: The grid convergence in the sup-norm.

6 Concluding remarks

In this paper, we have studied a nonlinear hyperbolic model describing the propagation and interaction of nonlinear waves on a Friedmann-Lemaître-Robertson-Walker back-

ground spacetime. We started from the relativistic Euler equations on a curved background and imposed a vanishing pressure in the expression of the energy-momentum tensor for perfect fluids. This led us to a geometric relativistic Burgers equation (see (1.2)) on the background spacetime under consideration. On a FLRW spacetime, Eq. (1.2) yields the model (3.3) of interest in the present work. The model involves a scaling factor $a=a(t)$ which depends on the so-called 'cosmic time' and a constant coefficient k, which can be normalized to take the values ± 1 or 0. The standard Burgers equation is recovered when $a(t)$ and k are chosen to vanish.

We have investigated nonlinear wave solutions to our model for the three possible values of the coefficient k. We compared numerical solutions for the cases $k=-1$, $k=0$ and $k=1$, and we found that the solution corresponding to $k=-1$ moves faster than the solution corresponding to $k=0$ and $k=1$ (Figs. 1,2,3 and 4). This can be explained from Eq. (3.3) by observing that the characteristic speed $\left(1-kr^2\right)^{1/2}$ is increased by decreasing k.

Our analysis relies on a proposed numerical discretization scheme which applies to weak solutions and is based on the finite volume technique. Our scheme is consistent with the conservative form of (the principal part of) our model and therefore correctly computes weak solutions. Our numerical experiments illustrate the convergence and efficiency of the proposed finite volume scheme for FLRW backgrounds. The finite volume methodology can be applied to the relativistic Burgers equation posed on other classes of background spacetimes. The advantages of such a rather simplified nonlinear hyperbolic model is that it allows one to develop and test numerical methods for weak solutions and reach definite conclusions concerning their convergence, efficiency, etc. Depending upon the particular background geometry, one want to guarantee that certain classes of solutions of particular interest are preserved by the scheme.

Acknowledgments

The first (T.C.) and third (B.O.) authors were supported by the Middle East Technical University (METU) through the grant BAP–08–11–2013–041 and by the Scientific and Technical Research Council of Turkey (TÜBİTAK) through the Ph.D. scholarship BIDEB 2214-A. The second author (PLF) was partially supported by the Innovative Training Networks (ITN) grant 642768 (ModCompShock).

References

[1] P. AMORIM, M. BEN-ARTZI, AND P.G. LEFLOCH, Hyperbolic conservation laws on manifolds: Total variation estimates and finite volume method, Meth. Appl. Analysis 12 (2005), 291–324.

[2] P. AMORIM, P.G. LEFLOCH, AND B. OKUTMUSTUR, Finite volume schemes on Lorentzian manifolds, Comm. Math. Sc. 6 (2008), 1059–1086.

[3] M. BEN-ARTZI, J. FALCOVITZ, AND P.G. LEFLOCH, Hyperbolic conservation laws on the sphere. A geometry-compatible finite volume scheme, J. Comput. Phys. 228 (2009), 5650–5668.
[4] M. BEN-ARTZI AND P.G. LEFLOCH, The well-posedness theory for geometry compatible hyperbolic conservation laws on manifolds, Ann. Inst. Henri Poincaré - Nonlinear Analysis 24 (2007), 989-1008.
[5] C. BERTHON, P.G. LEFLOCH, AND R. TURPAULT, Late-time/stiff-relaxation asymptotic-preserving approximations of hyperbolic equations, Math. of Comput. 82 (2013), 831–860.
[6] S. BOSCARINO, P.G. LEFLOCH, AND G. RUSSO, High–order asymptotic preserving methods for fully nonlinear relaxation problems, SIAM J. Sci. Comput. 36 (2014), 377–395.
[7] M. P. HOBSON, G. P. EFSTATHIOU, AND A. N. LASENBY, *General relativity. An introduction for physicists,* Cambridge University Press, 2006.
[8] S.N. KRUZKOV, First-order quasilinear equations in several independent variables, Mat. Sbornik 81 (1970), 285–355; English trans. in Math. USSR Sb. 10 (1970), 217–243.
[9] P.G. LEFLOCH, Structure-preserving shock-capturing methods: late-time asymptotics, curved geometry, small-scale dissipation, and nonconservative products, in "Lecture Notes of the XV 'Jacques-Louis Lions' Spanish-French School" Ed. C. Pars, C. Vázquez, and F. Coquel, SEMA SIMAI Springer Series, Springer Verlag, Switzerland, 2014, pp. 179–222.
[10] P.G. LEFLOCH AND H. MAKHLOF, A geometry-preserving finite volume method for compressible fluids on Schwarzschild spacetime, Commun. Comput. Phys. 15 (2014), 827–852.
[11] P.G. LEFLOCH, H. MAKHLOF, AND B. OKUTMUSTUR, Relativistic Burgers equations on a curved spacetime. Derivation and finite volume approximation, SIAM J. Num. Anal. 50 (2012), 2136–2158.
[12] P.G. LEFLOCH, W. NEVES, AND B. OKUTMUSTUR, Hyperbolic conservation laws on manifolds. Error estimate for finite volume schemes, Acta Math. Sinica 25 (2009), 1041–1066.
[13] G. RUSSO, Central schemes for conservation laws with application to shallow water equations, S. Rionero, G. Romano Ed., Trends and Applications of Mathematics to Mechanics: STAMM 2002, Springer Verlag, Italy, 2005, pp. 225–246.
[14] G. RUSSO, High-order shock-capturing schemes for balance laws, in Numerical solutions of partial differential equations, Adv. Courses Math. CRM Barcelona, Birkhäuser, Basel, 2009, pp. 59–147.
[15] B. VAN LEER, On the relation between the upwind-differencing schemes of Godunov, Engquist-Osher, and Roe, SIAM J. Sci. Stat. Comput. 5 (1984), 1–20.